

This article was downloaded by: [Tomsk State University of Control Systems and Radio]

On: 23 February 2013, At: 02:48

Publisher: Taylor & Francis

Informa Ltd Registered in England and Wales Registered Number: 1072954

Registered office: Mortimer House, 37-41 Mortimer Street, London W1T 3JH, UK



## Molecular Crystals and Liquid Crystals

Publication details, including instructions for authors and subscription information:

<http://www.tandfonline.com/loi/gmcl16>

## Electronic Excitations in Polyacetylene

S. Etemad<sup>a b</sup>, A. J. Heeger<sup>a b</sup>, L. Lauchlan<sup>a c</sup>, T.-C. Chung<sup>a d</sup> & A. G. Macdiarmid<sup>a d</sup>

<sup>a</sup> University of Pennsylvania, Philadelphia, Pa. 19104

<sup>b</sup> Department of Physics, Philadelphia, Pa. 19104

<sup>c</sup> Department of Material Science, Philadelphia, Pa. 19104

<sup>d</sup> Department of Chemistry, Philadelphia, Pa. 19104

Version of record first published: 19 Dec 2006.

To cite this article: S. Etemad, A. J. Heeger, L. Lauchlan, T.-C. Chung & A. G. Macdiarmid (1981): Electronic Excitations in Polyacetylene, *Molecular Crystals and Liquid Crystals*, 77:1-4, 43-63

To link to this article: <http://dx.doi.org/10.1080/00268948108075228>

PLEASE SCROLL DOWN FOR ARTICLE

Full terms and conditions of use: <http://www.tandfonline.com/page/terms-and-conditions>

This article may be used for research, teaching, and private study purposes. Any substantial or systematic reproduction, redistribution, reselling, loan, sub-licensing, systematic supply, or distribution in any form to anyone is expressly forbidden.

The publisher does not give any warranty express or implied or make any representation that the contents will be complete or accurate or up to date. The accuracy of any instructions, formulae, and drug doses should be

independently verified with primary sources. The publisher shall not be liable for any loss, actions, claims, proceedings, demand, or costs or damages whatsoever or howsoever caused arising directly or indirectly in connection with or arising out of the use of this material.

## ELECTRONIC EXCITATIONS IN POLYACETYLENE

S. ETEMAD<sup>+</sup>, A.J. HEEGER<sup>+</sup>, L. LAUCLAN<sup>++</sup>, T.-C. CHUNG<sup>\*</sup>  
A.G. MACDIARMID.<sup>\*</sup>  
University of Pennsylvania  
Philadelphia, Pa. 19104

Received for publication September 11, 1981

Recent experimental results on light scattering and absorption in polyacetylene are reviewed, and interpreted in terms of the soliton model. The data indicate that injection of an electron-electron (hole-hole) pair by chemical doping or photoinjection of an electron-hole pair invariably distort the lattice leading to formation of a soliton-antisoliton pair. It is concluded that unlike traditional semiconductors, the polyacetylene lattice is inherently unstable in the presence of electron and/or hole excitations.

## INTRODUCTION

The emergence of polymeric semiconductors as a new class of electronic materials has attracted considerable attention. The study of these systems has generated entirely new scientific concepts as well as potential for new technology. As polymers, these materials have a highly anisotropic quasi-one-dimensional electronic structure. This one-dimensionality makes such systems fundamentally different from conventional inorganic semiconductors. First, the enhanced phase space for the interaction of electrons and the lattice leads to a spontaneous symmetry breaking; i.e., the well known

<sup>+</sup> Department of Physics

<sup>++</sup> Department of Material Science

<sup>\*</sup> Department of Chemistry

Peierls instability. Second, theoretical analysis has shown that the electronic excitations invariably involve lattice distortions leading to formation of polaron and/or soliton excitations. Whereas polarons have analogues in 3-d semiconductors, solitons are nonlinear excitations peculiar to 1-d systems. As summarized in this review, the unusual features of such nonlinear excitations in polyacetylene, the prototype of these polymeric semiconductors, dramatically affect the physical properties of this material.

Polyacetylene is the simplest conjugated polymer<sup>1</sup>. It consists of weakly coupled chains of CH units forming a pseudo-one-dimensional lattice. Three of the four carbon valence electrons are in  $sp^2$  hybridized orbitals; two of the  $\sigma$ -type bonds construct the 1-d lattice while the third forms a bond with the hydrogen side group. The  $120^\circ$  bond angle between these three electrons can be satisfied by two possible arrangements of the carbons; trans-(CH)<sub>x</sub> and cis-(CH)<sub>x</sub> with two and four CH monomer per unit cell respectively (see Fig. 1).

In either isomer the remaining valence electron has the symmetry of a  $2p_z$  orbital with its charge density lobes perpendicular to the plane defined by the other three. In terms of an energy-band description, the  $\sigma$ -bonds form low-lying completely filled bands, while the  $\pi$ -bond corresponds to a half-filled conduction band provided all the bond lengths are equivalent. As a result of Peierls instability of the 1-d metal<sup>2</sup>, the bondlengths are not equivalent and alternate in size resulting in opening of an associated Peierls gap at the Fermi level.

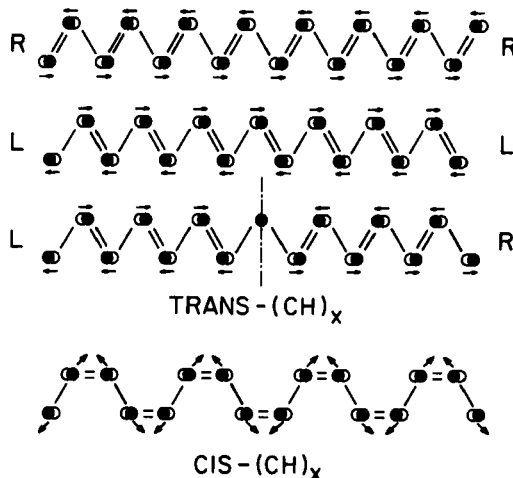


FIGURE 1 The possible arrangements of stable distortion patterns in  $(\text{CH})_x$ .

Simple estimates lead to a picture of polyacetylene as a broad band pseudo-one-dimensional semiconductor. In order to describe the Peierls distorted state we consider, as an initial approximation, a model in which the  $\pi$ -electrons of trans-(CH)<sub>x</sub> are treated in a tight binding approximation and the  $\sigma$ -electrons are assumed to move adiabatically with the nuclei. Let  $u_n$  be a configuration coordinate for displacement of the  $n$ th CH group along the molecular symmetry axis ( $x$ ), where  $u_n = 0$  for the undimerized chain. The Hamiltonian is

$$H = -\sum_{ns} [t_0 - \beta(u_{n+1} - u_n)] (c_{n+1,s}^+ c_{n,s} + \text{h.c.}) + \sum_n \frac{K}{2} (u_{n+1} - u_n)^2 + \sum_n \frac{M}{2} \dot{u}_n^2 \quad (1)$$

$M$  is the mass of the CH unit,  $K$  is the spring constant for the  $\sigma$ -energy when expanded to second order about the equilibrium undimerized systems,  $c_{ns}^+$  ( $c_{ns}$ ) creates (annihilates) a  $\pi$ -electron of spin  $s$  on the  $n$ th CH group, and  $\beta$  is the electron-phonon coupling constant. The zero temperature ground state of (1) correspond to a uniform dimerized state; i.e.

$$u_n = \pm(-1)^n u_0 \quad (2)$$

The transfer integral then reduces to  $t_{n+1,n} = t_0 \pm \frac{\Delta}{2}$  which alternates between double and single bonds and results in an associated Peierls gap of  $2\Delta = 8\beta u_0$ . The  $(\pm)$  in eq. (2) corresponds to the two possible degenerate structures; double bonds pointing "left" or "right" (see Fig. 1). The electronic structure of the uniformly distorted system is fully characterized by the two quantities,  $\Delta$  and  $t_0$ .

The overall bandwidth of the electronic states described by eq. (1) is  $4t_0 = 10$ - $12$  eV; whereas the energy gap  $2\Delta$  depends on the magnitude of the distortion. The recent analysis of X-ray scattering data from trans-(CH)<sub>x</sub> has shown a substantial distortion of magnitude  $u_0 \approx 0.03A$ .<sup>3</sup> The fact that this distortion can account for the observed energy gap of  $2\Delta = 1.5$  eV using a value for  $\beta$  in the accepted range (see section III) indicates that the Coulomb interactions do not play a dominant role. The basic validity of eq. (1) in defining the electronic structure of (CH)<sub>x</sub> is, therefore, justified. Within the context of eq.(1), solitons in trans-(CH)<sub>x</sub> are the natural nonlinear excitations of the system.

In this paper we review the results of recent light scattering and absorption experiments in cis- and trans-(CH)<sub>x</sub>. We show that the strong coupling of these nonlinear excitations to the electronic structure of the polymer leads directly to a number of unusual results which are fully compatible with the soliton model. The organization of this paper is as follows. In section II we review the relevant theoretical background, and the specific experimental evidence for presence of solitons in trans-(CH)<sub>x</sub>. In section III we review the results of optical absorption experiments which show that injection of an electron-electron (hole-hole) pair by chemical doping distorts the lattice leading to formation of a soliton-antisoliton pair. In section IV we study the photoexcitations in (CH)<sub>x</sub> using the recent photo-luminescence and photoconductivity results. It is shown that the existence of a broken symmetry degenerate ground state in trans- but not in cis-(CH)<sub>x</sub> has made a fundamental difference in their photoexcitations. In trans-(CH)<sub>x</sub> the photogenerated carriers are free soliton excitations, whereas in cis-(CH)<sub>x</sub> they are confined bipolarons. In section V it is concluded that unlike traditional semiconductors, the polyacetylene lattice is inherently unstable in the presence of electron and/or hole excitations.

## II SOLITONS IN POLYACETYLENE

There has been growing interest in the study of the physical properties of (CH)<sub>x</sub> due to the fact that the structure of trans-(CH)<sub>x</sub> exhibits a broken symmetry and has a two-fold degenerate ground state. (see Fig. 1) As a result, one expects soliton-like excitations, in the form of bond alternation domain walls, connecting the two degenerate phases. The properties of solitons in (CH)<sub>x</sub> have been explored theoretically in several papers<sup>4-8</sup>, which show that the coupling of these conformational excitations to the  $\pi$ -electrons leads to unusual electrical and magnetic properties. The possibility of experimental studies of such solitons in polyacetylene, therefore, represents a unique opportunity to explore nonlinear phenomena in condensed matter physics.

In an effort to characterize the soliton of polyacetylene, Su, Scheiffer, and Heeger (SSH) considered the two domains with "L" domain to the left and "R" domain to the right of a domain wall or soliton as shown in Fig. (1)<sup>7</sup>. They determined the properties of the soliton (creation energy, width, mass, spin, etc.) in terms of the microscopic parameters of equation (1) by minimizing the ground-state energy

of the system for a displacement pattern which reduces to the "L" and "R" phases as one moves to the far left or right. Using a staggered order parameter trial function  $\psi_n$ ,

$$\psi_n = (-1)^n u_0 \tanh(na/\xi) \quad (3)$$

they find that due to the competition between the elastic term (increases with a decrease in  $\xi$ ) and the condensation energy (increases with an increase in  $\xi$ ) the soliton in trans-(CH)<sub>x</sub> is spread over approximately 15 lattice sites. The analytic expression for  $\xi$  is  $2\xi = \frac{4t_0}{\Delta} \sim 15$ ; i.e. the soliton excitation is also characterized by  $\Delta$  and  $t_0$ .<sup>5,8</sup>

Associated with the soliton is a localized electronic state situated at mid-gap; i.e. half-way between the bonding valence band and the antibonding conduction band. SSH have pointed out that the solitons in trans-(CH)<sub>x</sub> are not the phase solitons which correspond to a 180° phase shift of the electronic charge-density wave, rather they are amplitude solitons with reversed charge-spin relations. As a result, if the localized state contains one electron the soliton is neutral, with spin  $\frac{1}{2}$ , and therefore is paramagnetic. On the other hand, if the localized state is empty (doubly occupied) the soliton is positively (negatively) charged, with spin 0, and non-magnetic. The soliton creation energy in trans-(CH)<sub>x</sub>; i.e., energy to generate a mid-gap state, is estimated by SSH to be  $E_s \sim .43$  eV which is less than half the gap,  $\Delta \sim .7$  eV. The analytical expression for  $E_s$  has been found to be

$$2E_s = \frac{4}{\pi} \Delta < 2\Delta \quad (4)$$

using the continuum limit approximation to the SSH model<sup>5,8</sup>. This result is of fundamental importance to the nature of the photoexcitations and the process of chemical doping in trans-(CH)<sub>x</sub>. Equation (4) clearly states that (within the model described by equation 1) from energetic considerations trans-(CH)<sub>x</sub> is unstable to the presence of an electron-hole (e-h) pair, or an e-e (h-h) pair in or near the conduction (valence) band, and distorts to form two mid-gap states of appropriate charge.

Specific evidence for the presence of neutral solitons in trans-(CH)<sub>x</sub> has emerged from studies of the spin dynamic by ESR linewidth studies,<sup>9</sup> by the observation of an Overhauser effect<sup>10</sup>, and through measurements of the frequency dependence of the nuclear spin-lattice relaxation rate,  $1/T_1$ .<sup>10,11</sup> The experimental results indicate the presence of highly

mobile spins, diffusing rapidly in one dimension. In a recent study of long time dynamics of this mobile spin Clark *et al.*<sup>11</sup> have shown that the 1-d diffusion persists uninterruptedly for at least as long as  $10^{-8}$  second.; i.e. when the 1-d motion is terminated by the crossover of spin to a neighbouring chain, or begins to sense the end of the chain. The fact that 1-d diffusion of the spin lasts for such a long time indicates that it is not associated with a free electron which has an interchain hopping rate of about  $t_1 \sim 10^{13}$  (sec<sup>-1</sup>).

Both the rapid motion along the chain and the remarkably long interchain cut-off times are expected for neutral solitons in trans-(CH)<sub>x</sub>. Since there is complete degeneracy (the soliton can be anywhere), and since the mass is small the soliton is expected to be highly mobile along the chain, but confined by topological constraints to move on a given chain. The magnitude of the soliton translational mass; i.e. the inertia of the bond alternation pattern and coupled electronic state to motion along the chain, was shown to be  $m_s \approx M(u_0^2/a\xi)$  (Ref.7). The enormous reduction in the soliton mass from the mass of a CH unit is due to the small amplitude of the bond alternation. Using the experimentally determined values of  $u_0$  and  $\xi$ , we estimate  $m_s \sim m_e$  where  $m_e$  is the electron mass.

### III SOLITON DOPING

#### (a) Effects on Lattice Dynamics:

Specific evidence for the formation of charged solitons upon doping has emerged from infrared studies of the donor and acceptor states in lightly doped polyacetylene. In a series of experiments with various dopants in both (CH)<sub>x</sub><sup>12</sup> and (CD)<sub>x</sub><sup>13</sup> it was found that upon dilute doping new absorption modes appeared in the IR region, with remarkable intensity. The doping induced modes are primarily polarized parallel to the chain direction and their intensities grow in proportion to the dopant level, becoming comparable to any of the intrinsic IR lines of the undoped polymer at about 0.1%. Thus the doping induced IR modes have oscillator strengths enhanced by approximately  $10^3$ ; such a large enhancement must arise from coupling of the new vibrational modes (induced by doping) to the electronic oscillator strength of the polyene chain. These results are quite general; the same modes can be observed for iodine and AsF<sub>5</sub> (p-type), and for Na doping (n-type)<sup>12</sup>.

Mele and Rice have been able to successfully interpret these results in terms of a theory of the lattice dynamics of solitons in trans-(CH)<sub>x</sub> or trans-(CD)<sub>x</sub><sup>14</sup>. In the frequency



range of the vibrational modes they have found several internal modes peculiar to the soliton structure. In particular, three of these modes were found to be strongly infrared active, deriving their oscillator strength from interactions with the  $\pi$ -electrons. They have shown that the dominant motions associated with the infrared active vibrational modes (IAVM) of a soliton involve an antisymmetric contraction of the single (or double) bonds on one side of the soliton center and an expansion on the other, thus driving charge back and forth across the soliton center. Due to the spatial spread of the soliton over about 15 sites, they find that the asymmetric oscillation of the electronic charge generates a large oscillating dipole moment consistent with the experimentally observed enhanced oscillator strength of the dopant induced IAVM.

The force field model constructed by Mele and Rice relied on a single adjustable parameter  $\beta$  which included the effect of nonlocal coupling of the atomic displacements through their interaction with the extended  $\pi$ -electronic states<sup>15</sup>. The value of  $\beta$  was determined by a fit of the calculated zone center frequencies of gerade modes to the observed Raman lines in unperturbed trans-(CH)<sub>x</sub> and (CD)<sub>x</sub>.<sup>13</sup> A comparison of the IAVM of solitons in trans-(CH)<sub>x</sub> and trans-(CD)<sub>x</sub> is shown in Fig. 2. The dashed curves are the experimental results for a concentration of approximately 0.1% and the solid curves are the result of the calculations with no adjustable parameter (the value of  $\beta = 6.9 \text{ eV/\AA}^0$  was already fixed). Besides the large frequency shifts upon deuteration, the detailed structure of the soliton IAVM that is driven by the higher frequency stretching oscillations is also changed.

As shown in Fig. 2, the calculated infrared absorption associated with the IAVM of solitons is in remarkably good agreement with the experimental results.<sup>13</sup> First, the frequencies are in agreement with the experimental results to an accuracy of a few percent for all the IAVM for both (CH)<sub>x</sub> and (CD)<sub>x</sub>. Secondly, the increased width and asymmetry of the higher frequency mode in (CD)<sub>x</sub> appears to be accounted for by the blue shifting of one of the degenerate modes in the low frequency line of trans-(CH)<sub>x</sub>. Finally, the calculated absolute integrated oscillator strengths correspond to  $\sim 20\%$  of the total associated with the added charge, and they agree with the experimental values to within a factor of 2-3. The relative oscillator strengths of the different modes are even more accurate. In (CH)<sub>x</sub>, the lower frequency mode is more intense, whereas in (CD)<sub>x</sub> we find that the higher frequency absorption is more intense. In both cases the experimental and theoretical intensity ratios are in close agreement.

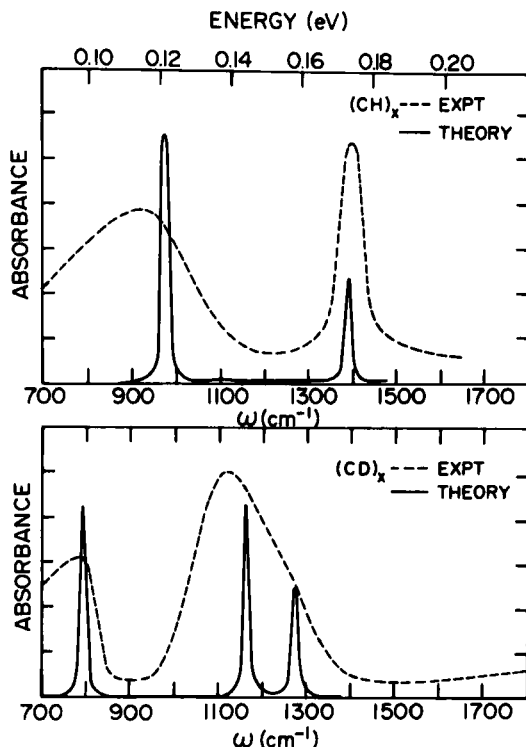


FIGURE 2 Comparison of the experimentally derived and the theoretically calculated additional absorption due to the infrared active vibrational modes (IAVM) of solitons in trans-(CH)<sub>x</sub> and trans-(CD)<sub>x</sub>. (Ref. 13)

(b) Effects on Bandstructure:

We shall now examine, from the point of view of electronic structure, the response of trans-(CH)<sub>x</sub> lattice to the presence of an electron-electron (hole-hole) pair in the conduction (valence) band. In contrast to the case of conventional semiconductors, we find that donor (acceptor) doping does not result in generation of localized states near the conduction (valence) band. Instead, independent of the nature of the dopant, addition or removal of electrons to or from the polymer chain is invariably accommodated by formation soliton induced localized states near mid-gap. Calculations of the absorption coefficient ( $\alpha$ ) show that a soliton kink on a chain suppresses the interband transition, whereas transitions involving the soliton level are found to have a significantly enhanced absorption cross-section. The results are in agreement with the experimental absorption spectra

obtained from trans-(CH)<sub>x</sub> lightly doped with AsF<sub>5</sub>.<sup>16</sup>

Takayama, Lin-Liu and Maki (TLM)<sup>8</sup> considered the continuum limit of the linear chain model introduced by SSH to describe (CH)<sub>x</sub>. Their analytical results are in agreement with the numerical results of SSH and allow explicit calculation of wave functions and matrix elements. Using TLM's formalism Suzuki et al<sup>16</sup> have calculated the various absorption coefficients and have compared the results with experiments. They find that for a perfect dimerized chain ( $\Delta(x) = \Delta_0$ ), the interband absorption coefficient (per carbon atom), for transitions from valence band (VB) to conduction band (CB), is

$$\alpha_1(\omega) = A f_1(\omega) \quad (5)$$

$$f_1(\omega) = \left(\frac{E_g}{\hbar\omega}\right)^2 \left[\left(\frac{\hbar\omega}{E_g}\right)^2 - 1\right]^{-1/2}$$

where  $A = (4\pi e^2 |M_x|^2) / m^2 n c^2 E_g$ ,  $E_g = 2\Delta_0$ ,  $e$  is the electron charge,  $c$  is the velocity of light, and  $n$  is the index of refraction. Although  $\alpha_1(\omega)$  diverges as  $(\hbar\omega - E_g)$ , this square root singularity will be smeared out by disorder, interchain coupling or fluctuations.

For a trans-(CH)<sub>x</sub> chain with a static kink ( $\Delta(x) = \Delta \tanh(x/\xi)$ ), the soliton formation energy takes the minimum value  $\frac{\pi}{2} \Delta$ , and one bound state appears at mid-gap. Using the results of TLM, Suzuki et al calculated  $\alpha_s$ , for transitions between a soliton level (S) and the band states to be

$$\alpha_s(\omega) = A \frac{\pi^2 \xi_0}{a} f_s(\omega) \quad (6)$$

$$f_s(\omega) = \left[\left(\frac{2\hbar\omega}{E_g}\right)^2 - 1\right]^{-1/2} \operatorname{sech}^2\left\{\frac{\pi}{2} \left[\left(\frac{2\hbar\omega}{E_g}\right)^2 - 1\right]^{1/2}\right\}$$

The factor  $(\pi^2 \xi_0 / a)$  in eq. (6) indicates an enhancement of the soliton transition resulting directly from the delocalization of the soliton wave function ( $\xi/a \gg 1$ ). For  $W = 10\text{eV}$  and  $E_g = 1.5\text{eV}$ , one finds  $\xi \sim 7a$  and  $(\pi^2 \xi/a) \sim 70$ . As a result, the transitions involving the soliton level should be observable even at extremely small concentrations. The interband  $\alpha_1(\omega)$  (per carbon atom) in the presence of a kink is correspondingly decreased and the overall oscillator strength is conserved. Suzuki et al in collaboration with Gammel and Krumhansl<sup>17</sup> originally obtained a uniform suppression of the absorption coefficient

$$\alpha'_1(\omega) = \alpha_1(\omega) \left(1 - \frac{\pi^2 \xi n^2}{2N} \frac{\xi}{a}\right) \quad (7)$$

for a chain with  $N$  (CH) units and one soliton at its center. More detailed recent calculations have shown that equation (7) is not exact<sup>18</sup>. The uniform suppression is, however, an excellent approximation in the frequency range  $\hbar\omega \geq 2.4\Delta$ , i.e., the frequency range of importance to experimental studies.<sup>16</sup> It is interesting to note that the presence of a soliton on a chain breaks the translational symmetry of the lattice. As a result, the momentum conserving (vertical) interband,<sup>16-18</sup> transition is quenched and  $\alpha_1$  is due to non-vertical terms.

The optical absorption spectra of  $\text{trans}-(\text{CH})_x$  are shown in Fig. 3.<sup>16</sup> Curves 1 through 5 on Fig. 3 show the effects of doping; 1-undoped, 2-very lightly doped with  $\text{AsF}_5$  (about 0.01%), 3-lightly doped with  $\text{AsF}_5$  (about 0.1%), and 4-subsequently compensated with  $\text{NH}_3$ ; all data are from the same (CH)<sub>x</sub> film. The doping was carried out *in situ* using extreme care<sup>x</sup> so that the results could be directly and quantitatively

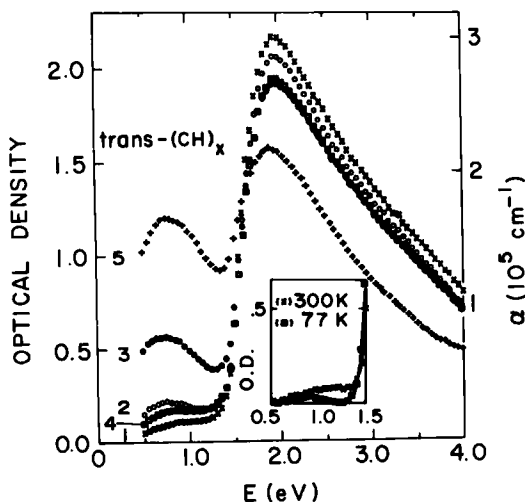


FIGURE 3 Absorption spectra of  $\text{trans}-(\text{CH})_x$ : curve 1, undoped; curve 2, 0.01%  $\text{AsF}_5$ ; curve 3, 0.1%  $\text{AsF}_5$ ; curve 4, compensated by  $\text{NH}_3$ ; and curve 5, 0.5%  $\text{AsF}_5$ . The inset shows the temperature dependence of  $\alpha(\omega)$  for undoped  $\text{trans}-(\text{CH})_x$ . (Ref. 16)

compared. Curve 5 on Fig. 3 was obtained with a separate film doped to a somewhat higher level (~.5%); quantitative comparison was possible through normalization of the absorption curve prior to doping. The effect of temperature on undoped (CH) is shown in the inset; data obtained at 77 K and 4.2 K are indistinguishable.

The strong absorption band with edge at 1.4 eV and peak at 1.95 eV has been attributed to the direct interband transition in a one-dimensional (1-d) band structure, and can be viewed as arising from a transition from the 1-d peak in the density of states in the valence band to that in the conduction band. The rounding appears to shift the position of the peaks in the VB and CB densities of states by about 0.2 eV. In addition to the main peak, a weak absorption (see the inset to Fig. 2) is observed centered near 0.9 eV, corresponding to a transition between the peak in VB density of states and a level inside the gap. Relative to the VB edge, the gap state occurs at about 0.7 eV; i.e., near mid-gap. On doping with AsF<sub>5</sub> the "mid-gap" absorption grows with increasing concentration and shifts slightly towards lower energies.

The characteristic features of the "mid-gap" and main absorption bands can be explained if we assume that the doping proceeds through formation of positive charged solitons ( $S^+$ ) and that the low energy absorption band is associated with the transition from the valence band into the  $S^+$  level to form a neutral soliton ( $S^0$ ). The low energy absorption, seen in the low temperature data of inset to Fig. (3), indicates that soliton states are also present in the undoped material. As the number of  $S^+$  increases with AsF<sub>5</sub> doping, the strength of the low energy transition ( $S^+ + e \rightarrow S^0$ ) grows proportionally. Further, the calculations presented above predict that the interband transition will be uniformly suppressed with the introduction of soliton kinks, again in agreement with the experimental results. Making a quantitative comparison, the integrated intensity of the low energy absorption band after 0.1% doping (curve 3) is about one tenth of that of the main absorption band of the undoped sample. We infer from eq. 6 a value for  $\pi^2(\xi/a) \sim 10^2$  in good agreement with the theoretical value. The uniform decrease in intensity of the interband transition is also evident in curve 3 and corresponds to about a 10% reduction relative to the undoped sample.

#### IV PHOTOEXCITATIONS IN POLYACETYLENE

Interest in photoexcitation studies of  $(\text{CH})_x$  has been stimulated by the recent calculations of Su and Schreiffer<sup>19</sup>, who considered direct injection of an e-h pair and studied the time evolution of the system. Their principal result was the conclusion that in trans- $(\text{CH})_x$  a photo-injected e-h pair evolves to a soliton-antisoliton pair in a time of order of the reciprocal of an optical phonon frequency. This is the central experimental question addressed in this section: Are solitons photogenerated in polyacetylene? The proposed photogeneration of charged solitons<sup>20</sup> has clear implications which can be checked through studies of photoluminescence and photoconductivity. We therefore present and discuss in this section the experimental results obtained with these two complementary techniques in cis- and trans- $(\text{CH})_x$ .

In the scattered light spectrum from cis- $(\text{CH})_x$ , we find a relatively broad luminescence structure peaking at 1.9 eV, near the interband absorption edge, together with a series of multiple order Raman lines<sup>21-22</sup> (see Fig. 4). Through a measurements of the excitation spectrum, we have found that the luminescence turns on sharply for excitation energies greater than 2.05 eV. The luminescence structure (corrected for self absorption effect) is compared with its excitation spectrum and the absorption coefficient of cis- $(\text{CH})_x$  in Fig. 5. The luminescence appears to consist of either a broad single line or a distribution Stokes shifted emissions as deep as 0.6 eV inside the gap. The luminescence intensity is essentially independent of temperature from 7K to room temperature.

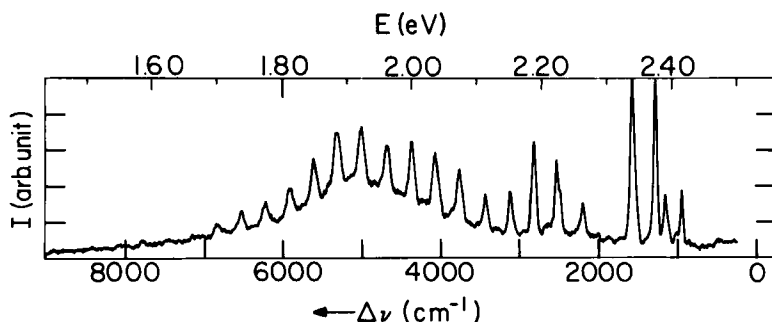


FIGURE 4 Scattered light spectrum from cis- $(\text{CH})_x$  showing multiple overtone Raman structure superimposed on a broad luminescence background.

Isomerization of the same sample to  $\text{trans}-(\text{CH})_x$  quenches the luminescence; we find no indication of luminescence near the interband absorption edge of  $\text{trans}-(\text{CH})_x$  even at temperatures as low as 7 K.<sup>22</sup> Recent experiments have confirmed<sup>23</sup> that any luminescence from  $\text{trans}-(\text{CH})_x$  in the region from mid-gap to bandedge is at least two orders of magnitude smaller than the result from  $\text{cis}-(\text{CH})_x$  shown in Fig. 4. It appears then the absence of bandedge luminescence in  $\text{trans}-(\text{CH})_x$  is not due to the presence of a large Stokes shift.

The photocurrent ( $I_{\text{ph}}$ ) spectrum for  $\text{trans}-(\text{CH})_x$  is plotted in Fig. 6 and compared with the energy dependence of the absorption spectrum for  $\text{trans}-(\text{CH})_x$ ,  $\alpha_t(\omega)$ .<sup>24</sup>  $I_{\text{ph}}$  has a threshold at 1.0 eV, well below the interband absorption edge at 1.5 eV, implying the presence of states deep inside the gap. This is clearly shown in the inset to Fig. 6 where the photoresponse and absorption are compared on a linear scale. The threshold for the generation of free carriers is better seen in the logarithmic plot of  $I_{\text{ph}}$  versus photon energy (Fig. 6). The absence of structure in  $\alpha_t(\omega)$  at the onset of  $I_{\text{ph}}$  implies a low quantum efficiency at threshold. The free carrier generation efficiency rises exponentially above the threshold and changes to a slow increase above the onset of the interband transition. We also note the absence of any

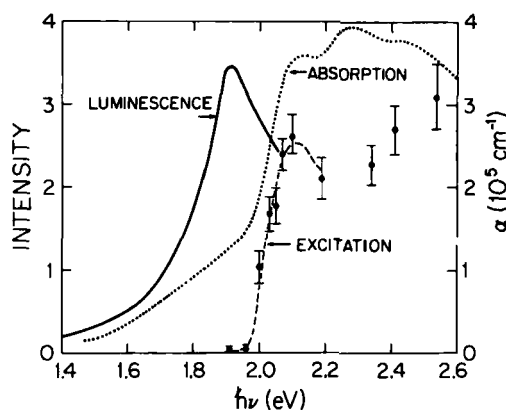


FIGURE 5 The luminescence spectrum of  $\text{cis}-(\text{CH})_x$  compared with the excitation and a typical absorption spectra.

structure in  $I_{ph}$  near the sharp onset of the interband transition, indicating the photocurrent in  $\text{trans}-(\text{CH})_x$  is not determined by surface dissociation of excitons that might also quench luminescence.

Measurements of  $I_{ph}$  in  $\text{cis}-(\text{CH})_x$  were also attempted. Under similar conditions any photoresponse in samples of 95%  $\text{cis}$ -rich  $(\text{CH})_x$  was below the noise level of our experiment. The upper limit on  $I_{ph}$  in  $\text{cis}-(\text{CH})_x$  is more than three orders of magnitude smaller than  $I_{ph}$  in  $\text{trans}-(\text{CH})_x$ . *In situ* isomerization of the same film resulted in the sizeable  $I_{ph}$  shown in Fig. 6. As detailed elsewhere, bolometric effects play no role in the photoconductivity results summarized here.<sup>24</sup>

In traditional semiconductors, photoconductivity and recombination luminescence are intimately related, and both are observed after photoexcitation. Photoconductivity indicates the presence of free carriers generated by the absorbed photons. Although the subsequent recombination of these photogenerated carriers can take place either radiatively or non-radiatively, recombination luminescence is commonly observed, at least at low temperatures. The fundamental

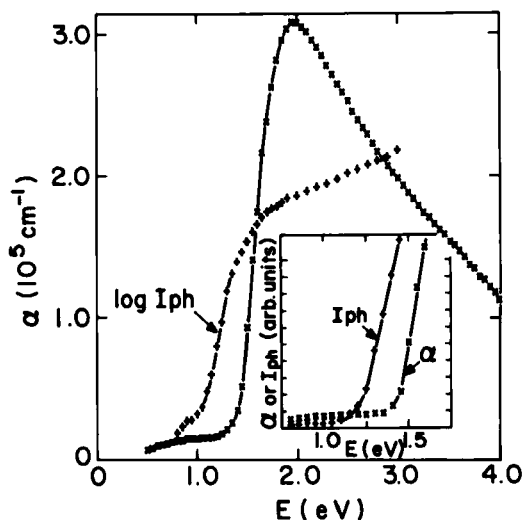


FIGURE 6 The photocurrent ( $I_{ph}$ ) and absorption ( $\alpha$ ) spectra of  $\text{trans}-(\text{CH})_x$ .  $I_{ph}$  and  $\alpha_t$  are compared on a linear scale in the inset. (Ref. 24)



differences between such traditional data and those obtained from polyacetylene can be seen by comparison of the  $(\text{CH})_x$  results with results obtained from cadmium sulfide ( $\text{CdS}$ ) $_x$ . The luminescence and multiple order Raman scattering data from  $\text{CdS}$ <sup>25</sup> are similar to the results obtained from cis- $(\text{CH})_x$ . However, in  $\text{CdS}$ , a strong photoconductive response is observed for photon energies just above the band edge,<sup>26</sup> whereas in cis- $(\text{CH})_x$  significant photogeneration of free carriers is not observed even for photon energies 1 eV above the band edge.

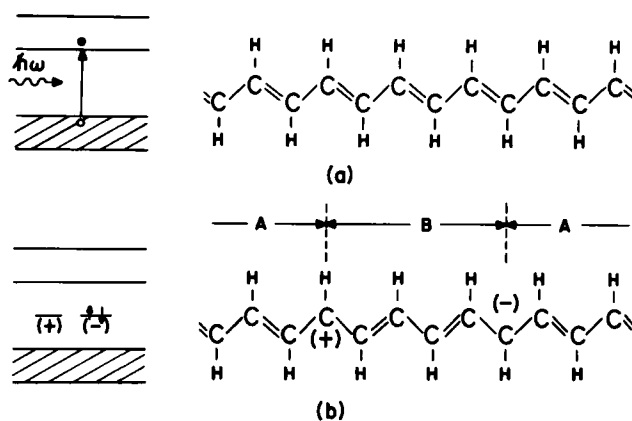


FIGURE 7a. Band diagram and chemical structure diagram for trans- $(\text{CH})_x$ . The band diagram shows schematically the absorption of a photon and the creation of an e-h pair. b. A trans- $(\text{CH})_x$  chain containing a charged soliton-antisoliton pair. Since regions A and B are degenerate, the solitons are free and can move apart with no cost in energy. The corresponding band diagram shows the mid-gap states associated with the two solitons; one empty (+) and the other double occupied (-).

Isomerization to trans-(CH)<sub>x</sub> quenches the luminescence at all temperatures, but turns on the photoconductivity. In neither isomer is the traditional combination of effects observed. These unique experimental results, therefore, lead us to consider the proposed photogeneration of solitons in more detail.

A schematic diagram of the photogeneration of a charged soliton-antisoliton pair in trans-(CH)<sub>x</sub> is shown in Fig. 7. The incident photon (for  $h\nu \geq 2\Delta$ ) generates an e-h pair within the rigid lattice (Fig. 7a). The system rapidly evolves to a charged soliton pair (Fig. 7b) as shown by Su and Schrieffer. After a time of order  $10^{-13}$  sec, their results imply the presence of two kinks separating degenerate regions. Because of the precise degeneracy of the A and B phases, the two charged solitons are free to move in an applied electric field and contribute to the photoconductivity. The simultaneous absence

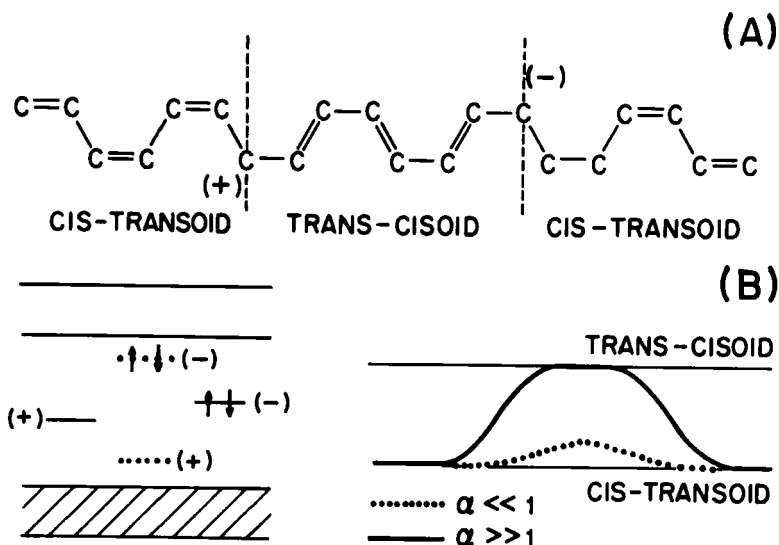


FIGURE 8(A) Chemical structure of cis-(CH)<sub>x</sub> containing a charged soliton-antisoliton pair. (B) The spatial variation of the order parameter (eq. 10) and the corresponding electronic state inside the gap for the two limiting case of weak ( $\alpha \gg 1$ ) and strong ( $\alpha \ll 1$ ) confinement.

of band edge luminescence in trans-(CH)<sub>x</sub> even at lowest temperatures is consistent with the proposed photogeneration of charged soliton-antisoliton pairs. In this case, band edge luminescence cannot occur since there are no electrons and holes. The charged carrier pair consists of two kinks with associated mid-gap states which cannot give rise to band edge luminescence.

The topological degeneracy in trans-(CH)<sub>x</sub> is not present in cis-(CH)<sub>x</sub>, so that soliton photogeneration<sup>x</sup> would not lead to photoconductivity in the cis-isomer. Since the cis-transoid configuration has a lower energy than the trans-cisoid configuration, domain walls would separate non-degenerate regions (Fig. 8A). Consider the photoexcitation of a charged soliton-antisoliton pair as shown schematically in Fig. 8A. The energy required is

$$E_{\text{tot}} = 2E_s + n \Delta E_0 \quad (8)$$

where  $E_s$  is the energy for creation of a single soliton (analogous to the soliton creation energy in trans-(CH)<sub>x</sub>),  $n$  is the number of CH monomers separating the two kinks, and  $\Delta E_0$  is the energy difference between cis-transoid and trans-cisoid configurations (Fig. 8A), expected to be a small fraction of the full gap  $2\Delta \sim 2.0$  eV in cis-(CH)<sub>x</sub>. Thus, as they begin to form, the two solitons would be "confined", or bound into a polaron-like entity; the farther apart, the greater the energy. As a result, one expects the photogenerated pair to quickly recombine, thereby, quenching the photoconductivity in cis-(CH)<sub>x</sub>.

The unusual combination of photoconductivity and luminescence results in cis- and trans-(CH)<sub>x</sub> exist in spite of the close similarity of their microscopic structure. In particular the absorption spectra of the two isomers (see Fig. 5 and 6) are quite similar. We, therefore, do not expect any major change in the electronic interaction upon isomerization. We should also note that within the next-nearest-neighbour approximation the two isomers are identical. The unusual changes seen in the photoresponse and scattered light spectrum upon isomerization of cis-(CH)<sub>x</sub> to trans-(CH)<sub>x</sub> are the result of change in symmetry of the polymer and not to some extrinsic effects. Thus, the observation of luminescence in cis-(CH)<sub>x</sub> but not in trans-(CH)<sub>x</sub>, and the observation of photoconductivity in trans-(CH)<sub>x</sub> but not in cis-(CH)<sub>x</sub> provide confirmation of the proposal that solitons are the photogenerated carriers. In trans-(CH)<sub>x</sub>, the degenerate ground state leads to free soliton excitations, absence of the band edge lumin-

escence and photoconductivity. In cis-(CH)<sub>x</sub> the non-degenerate ground state leads to confinement of the photogenerated carriers, absence of photoconductivity, and to the observed recombination luminescence.

The luminescence results in cis-(CH)<sub>x</sub> as shown in Figs. 4, 5 provide some insight into the dynamics of the system. The energy given off to photons during the formation of the lattice distortion would lead to a Stokes shift of the luminescence relative to the minimum energy needed to make a free e-h pair. Viewing the luminescence as a single broad peak (rather than a distribution of emissions), a Stokes shift of  $\Delta E_s = 0.15$  eV is observed relative to the onset of photoexcitation at 2.05 eV (see Fig. 5). The magnitude of  $\Delta E_s$  is, however, much less than that expected for the complete formation of either two free solitons or two free polarons. In the case of two free solitons, the corresponding electronic levels would be near mid-gap with the luminescence energy going to zero in the limit of  $(\Delta E_0/2\Delta) \rightarrow 0$ . In this limit for a well-separated electron-polaron and hole-polaron<sup>27-28</sup> the corresponding luminescence energy would be  $\hbar\omega_y = \sqrt{2}\Delta = 1.4\Delta$  with an implied Stokes shift of  $\Delta E_s = .6\Delta$ . The much smaller experimental value of  $\Delta E_s \sim .07\Delta$ , therefore, indicates that the absence of a degenerate ground state in cis-(CH)<sub>x</sub> has made qualitative changes in the dynamics of photoexcitations in the two isomers.

Brazovskii and Kirova<sup>27</sup> have pointed out that because of the confinement energy (eq. 8) the total gap in a commensurate Peierls distorted system arises from a sum of two terms,

$$\Delta(x) = \Delta_i(x) + \Delta_e \quad (9)$$

where  $\Delta_i(x)$  is the intrinsic Peierls gap stabilized by  $\pi$ -electrons, and  $\Delta_e$  is the incompressible contribution arising from the  $\sigma$ -electron backbone structure. In trans-(CH)<sub>x</sub>,  $\Delta_e = 0$  by symmetry; whereas in cis-(CH)<sub>x</sub>  $\Delta_e \neq 0$  since even in the case of equal bondlengths the transfer integrals alternate. The increase in the optical gap of cis-(CH)<sub>x</sub> compared with that of trans-(CH)<sub>x</sub> implies a relatively large  $\Delta_e$ .

Using this ansatz, Brazowski and Kirova defined the basic confinement parameter  $\gamma = \Delta_e/\lambda\Delta$  (where  $\lambda$  is the electron-phonon coupling constant) and developed a detailed theory of the excited states in the presence of confinement. For cis-(CH)<sub>x</sub>, they find for the gap parameter  $\Delta(x) = (1-\delta(x))$

$$\delta(x) = \tanh\alpha [\tanh(x/\xi^* + \alpha/2) - \tanh(x/\xi^* - \alpha/2)] \quad (10)$$

where  $\alpha$  is a variable which depends on  $\Delta_e$  and  $\Delta_i$  and is fixed by minimizing the total bi-polaron energy, and  $\xi^* = \xi \cosh \alpha$  with  $\xi = 2t_0/\Delta \approx 7a$ . For weak confinement ( $\alpha \gg 1$ ) the excitation is equivalent to two well separated domain walls; for strong confinement ( $\alpha \ll 1$ ) eq. 10 describes a shallow bi-polaron. (see Fig. 8B) On formation of the excitation, two electronic states are pulled inside the gap at  $E = \pm \Delta/\cosh \alpha$  relative to the gap center. If we assume<sup>p</sup> that in cis-(CH)<sub>x</sub> the optical excitation quickly comes to the minimum energy configuration described by eq. 10 then the luminescence would occur at  $\hbar\omega_p = 2\Delta/\cosh \alpha$ , and the Stokes shift would be  $\Delta E_s = 2\Delta(1-1/\cosh \alpha)$ . Using the experimental value,  $\Delta E_s = 0.15\Delta_s$ , we obtain  $\alpha = 0.4$  and  $\gamma \approx 2.8$  implying very strong confinement ( $\Delta \gg \Delta_i$ ) and/or a much smaller  $\lambda$  in cis- than in trans-(CH)<sub>x</sub>. Both results are contrary to expectation and indicate that the peak in luminescence does not correspond to the position of a localized electronic state in quasiequilibrium with the lattice. The unusual combination of a broad luminescence structure together with a very small Stokes shift can then arise from the dynamics of the localized electronic state inside the gap (see Fig. 8B) before coming to its quasiequilibrium at the minimum energy configuration. As suggested by Brazovskii, the luminescence is then due to a distribution of emission (corresponding to confined soliton-antisoliton pairs in various states of internal phonon excitation) with the quasiequilibrium luminescence indicated by the low energy tail.<sup>29</sup> Assuming  $2\Delta \approx 0.5$  eV and  $\lambda \approx 0.4$  (as implied by the difference in the optical gaps of cis  $\lambda$  and trans isomers and the relation  $\Delta \approx 2t_0 e^{-1/\lambda}$ ) the confinement parameter is  $\gamma = 0.6$ , leading to a value of  $\alpha = 1$ . This value of  $\alpha$  would imply the luminescence tail ends for energies near  $\sim 1.3$  eV, in reasonable agreement with the result of Figs. 4 and 5. The corresponding bipolaron, when in quasiequilibrium with the lattice, would have a width of  $\xi^* = 1.3\xi \approx 20a$ , and a maximum depth of  $\delta(0) \sim 0.7\Delta$  in the order parameter defined by eq. 10.

## V CONCLUSION

The experimental results reviewed in this paper show that not only are solitons present in polyacetylene but they are the primary electronic excitations of the coupled electron-lattice

in this semiconducting polymer. From the appearance of the characteristic infrared active vibrational modes of a charged domain wall concurrent with the enhanced mid-gap absorption upon doping, it is concluded that doping in trans-(CH)<sub>x</sub> proceeds through formation of solitons. To avoid possible complexities associated with soliton generation by chemical doping we have also considered experimental configurations that have permitted us to study the response of the lattice to direct photo-injection of e-h pairs. The existence of the two isomers of polyacetylene has provided the conceptual and experimental basis for the study of the photoexcitations in the undoped polymer in terms of photogeneration of solitons. Thus, injection of an electron-electron (hole-hole) pair by chemical doping or photoinjection of an electron-hole pair distort the lattice leading to formation of a soliton-anti-soliton pair.

The theoretical interpretation of the experimental results has been based on a simple 1-d Hamiltonian, which describes the Peierls distortion in a system of noninteracting electrons with strong coupling to the lattice. Solitons are the natural nonlinear excitations of such a system. As a result, unlike the traditional semiconductors, where electrons and holes can be stable excitations, in polyacetylene the lattice is inherently unstable to their presence.

#### ACKNOWLEDGEMENTS

The experimental confirmation of soliton doping discussed in section III is a result of fruitful collaborations with Dr. J. Mele, Dr. M.J. Rice and Dr. A. Pron (Ref. 13), and N. Suzuki and M. Ozaki (Ref. 16). We thank Dr. S. Brazovskii, Prof. J.R. Schrieffer and Dr. S. Kivelson for several enlightening discussions. This review was prepared under support from the Army Research Office (DAAG29-81-K-0058).

#### REFERENCES

1. A.J. Heeger, and A.G. MacDiarmid, The Physics and Chemistry of Low Dimensional Solids Ed. by Louis Alcacer (D. Reidel Publishing Co., 1980) p. 353.
2. J.T. Devreese, R.P. Evrard, and V.E. van Doren (Plenum Press, N.Y. 1978) Highly Conducting One-Dimensional Solids, contains several reviews on this topic.
3. C. Fincher, C.E. Chen, A.J. Heeger, J.B. Hastings and A.G. MacDiarmid (these proceedings).

4. J.A. Pople and J.H. Walmsley, *Mol. Phys.* 5, 15 (1962).
5. S. Brazovskii, *JETP Lett.* 28, 656 (1978); *ibid.* *JETP* 78, 677 (1980).
6. M.J. Rice, *Phys. Lett.* 71A, 152 (1979).
7. W.P. Su, J.R. Schrieffer, and A.J. Heeger, *Phys. Rev. Lett.* 42, 1698 (1979); *ibid.* *Phys. Rev. B* 22, 2099 (1980).
8. H. Takayama, Y.R. Lin-Liu and K. Maki, *Phys. Rev. B* 21, 2388 (1980).
9. B.R. Weinberger, E. Ehrenfreund, A. Pron, A.H. Heeger and A.G. MacDiarmid, *J. Chem. Phys.* 72, 4749 (1980).
10. M. Nechtschein, F. Devreux, R.L. Greene, T.C. Clarke, and G.B. Street, *Phys. Rev. Lett.* 44, 356 (1980).
11. W.G. Clark, K. Gloves, J. Sammy, C. Murayana, S. Etemad, and M. Maxfield, (these proceedings).
12. C.R. Fincher Jr., M. Ozaki, A.J. Heeger, and A.G. MacDiarmid, *Phys. Rev. B* 19, 4140 (1979).
13. S. Etemad, A. Pron, A.J. Heeger, A.G. MacDiarmid, F.J. Mele, and M.J. Rice, *Phys. Rev. B* 23, 5137 (1981).
14. E.J. Mele, and M.J. Rice, *Phys. Rev. Lett.* 45, 926 (1980).
15. E.J. Mele, and M.J. Rice, *Solid State Commun.* 34, 339 (1980).
16. N. Suzuki, M. Ozaki, S. Etemad, A.J. Heeger, and A.G. MacDiarmid, *Phys. Rev. Lett.* 45, 1209 (1980); Erratum *Phys. Rev. Lett.* 45, 1483, (1980).
17. J. Tinka Gammel and J.A. Krumhansl, preprint (1980).
18. S. Kivelson, T.-K. Lee, Y.R. Lin-Liu, I. Peschel, and L. Yu, preprint (1981).
19. W.P. Su and J.R. Schrieffer, *Proc. Nat. Acad. of Sci.* 77, 5626 (1980).
20. S. Etemad, M. Ozaki, A.J. Heeger, and A.G. MacDiarmid, *Proc. of the "International Conf. on Low Dimensional Synthetic Metal,"* Helsingor, Denmark, August 1980, *Chemica Scripta* 17, 159 (1981).
21. L.S. Lichtmann, A. Sarhangi, D.C. Fitchen, *Solid State Commun.* 36, 869 (1980).
22. L. Lauchlan, S. Etemad, T.-C. Chung, A.J. Heeger, and A.G. MacDiarmid, *Phys. Rev. B* 24, 1 (1981).
23. J. Orenstein, private communication.
24. S. Etemad, M. Mitani, M. Ozaki, T.-C. Chung, A.J. Heeger and A.G. MacDiarmid, *Solid State Commun.* 40, 75 (1981).
25. R.C.C. Leite, J.F. Scott, and T.C. Damen, *Phys. Rev. Lett.* 22, 782 (1969); M.V. Klein, S.P.S. Porto, *Phys. Rev. Lett.* 22, 782 (1969).
26. See, for example R.H. Bube, *Photoconductivity of Solids*, Wiley and Sons, N.Y. 1960, p. 230 and 391.
27. S. Brazovskii and N. Kirova, *JETP Lett.* Jan. (1981).
28. D.K. Campbell and A. Bishop, *Phys. Rev. B* (in press).
29. S. Brazovskii, private communication.